Finite-time scaling via linear driving: Application to the two-dimensional Potts model

Xianzhi Huang, Shurong Gong, Fan Zhong,* and Shuangli Fan

State Key Laboratory of Optoelectronic Materials and Technologies, School of Physics and Engineering, Zhongshan University, Guangzhou 510275, People's Republic of China

We apply finite-time scaling to the q-state Potts model with $q=3$ and 4 on two-dimensional lattices to determine its critical properties. This consists in applying to the model a linearly varying external field that couples to one of its q states to manipulate its dynamics in the vicinity of its criticality and that drives the system out of equilibrium and thus produces hysteresis and in defining an order parameter other than the usual one and a nonequilibrium susceptibility to extract coercive fields. From the finite-time scaling of the order parameter, the coercivity, and the hysteresis area and its derivative, we are able to determine systematically both static and dynamic critical exponents as well as the critical temperature. The static critical exponents obtained in general and the magnetic exponent δ in particular agree reasonably with the conjectured ones. The dynamic critical exponents obtained appear to confirm the proposed dynamic weak universality but unlikely to agree with recent short-time dynamic results for $q=4$. Our results also suggest an alternative way to characterize the weak universality.

I. INTRODUCTION

Numerical simulations have become indispensable for studying critical phenomena whose hallmark is a diverging correlation length. They are carried out inevitably, however, on finite systems, although real phase transitions occur only at the thermodynamic limit. Yet, this nuisance has turned into a blessing. The method of finite-size scaling (FSS) has become a routine to extract critical properties from numerical simulations of finite systems [1–3]. Under the assumption that upon a renormalization-group (RG) transformation of a length rescaling factor b, the coupling constants of a finite lattice transform in the same way as in the thermodynamics limit, the singular part of the free energy of a finite lattice then transforms as

$$F(\tau,H,L^{-1}) = b^{-d}F(\tau b^{1/\nu},Hb^{\beta\delta/\nu},bL^{-1}), \tag{1}$$

where δ, β, and ν are critical exponents, L is a characteristic length scale of the system, d is the spatial dimension, H is the external magnetic field, and the reduced temperature $\tau = (T-T_c)/T_c$, with T_c being the critical temperature. As a result, one arrives at the FSS ansatz for the free energy

$$F(\tau,H,L^{-1}) = L^{-d}f(\tau L^{1/\nu},HL^{\beta\delta/\nu}), \tag{2}$$

where f is a scaling function. We have neglected possible dimensional factors for conciseness hereafter. Appropriate differentiations of Eq. (2) then give rise to corresponding scaling forms for the magnetization M and the susceptibility χ, viz.,

$$M(\tau,L) = L^{-\beta/\nu}f_1(\tau L^{1/\nu}), \tag{3a}$$

$$\chi(\tau,L) = L^{\gamma/\nu}f_2(\tau L^{1/\nu}), \tag{3b}$$

where γ is a critical exponent and the fs are all scaling functions. In terms of the infinite system correlation length ξ_∞

that diverges at T_c as $\xi_\infty \sim |\tau|^{-\nu}$, the argument of fs in Eqs. (2) is proportional to L/ξ_∞ that governs the finite-size behavior; for small L/ξ_∞ FSS appears in which L is a relevant length scale, while large L/ξ_∞ is the thermodynamic limit in which equilibrium behavior shows and L is irrelevant. Note that all the critical exponents assume their infinite lattices values due to the assumption [4]. Consequently, measuring the thermodynamics quantities for a series of L can then determine the corresponding exponent ratios since pure power laws emerge exactly at T_c or $\tau=0$ at which fs are assumed to be regular. In fact, for too small systems and temperatures away from T_c, corrections to scaling have to be taken into account. Nevertheless, delicate methods exist for extracting critical exponents as well as T_c [2,3].

Noting the effectiveness of the FSS, we systematically proposed recently its dynamic counterpart, finite-time scaling (FTS) by noting that the equilibrium relaxation time t_{eq} also diverges at T_c and dynamic scaling follows accordingly [5]. This scaling consists in imposing an external time scale to a system to manipulate its dynamics via an applied external field that is varying linearly with time with a rate of R. We have argued that it is the inverse sweep rate of the field, R^{-1}, that serves as an analog of the controllable finite size scale to govern the dynamic scaling of the system in the FTS regime. In particular, we have shown that for $H=Rt$, the magnetization transforms under a rescaling of factor b as

$$M(\tau,H,R) = b^{-\beta/\nu}M(\tau b^{1/\nu},Hb^{\beta\delta/\nu},Rb^{r_H}), \tag{4}$$

so that the finite-time scaled equation of state is

$$M(\tau,H,R) = R^{\beta/\nu r_H}g(\tau R^{-1/\nu r_H},HR^{-\beta\delta/\nu r_H}), \tag{5}$$

in close similarity with Eq. (3a) but without setting $H=0$ by noting that the RG eigenvalue of R is [6]

$$r_H = z + \beta\delta/\nu \tag{6}$$

instead of 1 for L, where g is a scaling function and z the dynamic critical exponent. As a consequence, the FTS regime is defined by small $|\tau|R^{-1/\nu r_H}$ or an intrinsic relaxation

*Corresponding author; stszf@mail.sysu.edu.cn

time $t_{eq} \sim \xi_{\infty}^z \gtrsim H_{eq}R^{-1}$ (the factor $H_{eq} \sim M_{eq}^{\delta} \sim |\tau|^{\beta\delta}$ is the equilibrium magnetic field corresponding to the equilibrium magnetization M_{eq} at $\tau < 0$ and sets the dimension right), while for large $|\tau|R^{-1/\nu r_H}$ or small $R \ll |\tau|^{\nu r_H} \sim H_{eq}/t_{eq}$, the field varies so slowly that although it is changing, before it changes, the system has already equilibrated so that the usual equilibrium scaling

$$M(\tau, H) = \tau^{\beta} g_1 (H \tau^{-\beta\delta}), \tag{7}$$

emerges, where g_1 is another scaling function. R cannot be, of course, too large otherwise the system under driving will leave the critical region considered. It is remarkable that all critical exponents in FTS are naturally identical with the usual infinite time systems without the above assumption for FSS [5]. A systematic method for determining both dynamic and static critical exponents as well as the critical point has then been developed out of Eq. (5) through the scaling of hysteresis areas and coercive fields and testified favorably with two-dimensional (2D) and three-dimensional Ising models [5]. Moreover, due to the finite time scale, critical slowing down does not appear but is converted into visible processes as compared to its spatial counterpart even though measurements are also performed at T_c. Here we shall apply the method to the 2D Potts model to show its versatility.

The Potts model [7–9] is a direct generalization of the Ising model to the case in which each spin can take on q possible states. It has been rigorously proved that the 2D Potts model exhibits continuous phase transitions for $q \leq 4$ and first-order transitions otherwise [10]. The transition point of the model is exactly known from self-duality for a general q [8]. The thermal [11] and magnetic [12] RG eigenvalues for $q \leq 4$ have been proposed hypothetically; and the predicted critical exponents for $q=3$ and 4 agree with the exact exponents [13,14] of the hard-hexagonal lattice gas [15] and the Baxter-Wu model [16], which are believed to be in the same universality class to the $q=3$ and $q=4$ Potts model, respectively. Conformal-invariance theory also gives rise to the exact exponents that are identified with the Potts model [17]. In addition, the conjectures were shown to be asymptotically exact [18] and verified by a FSS combined with a transfer matrix technique for continuous q and were suggested to be true for $q=3$ and 4 [19]. Early numerical results (see Table III below for detailed values) for the critical exponents such as β and ν including series expansions and real-space RG as summarized in the review paper [8] conformed with the conjectured values for $q=3$ and 4; but with larger deviations for the latter presumably because of the presence of strong logarithmic singularity [20,21]. Recent results are more accurate as critical slowing down can be avoided [21–29].

A particular critical exponent that is of concern here is the magnetic exponent δ. The conjectured values for the 2D Potts model are 14 and 15 for $q=3$ and 4, respectively. However, numerical results that measure it in the presence of an external field so far are not as good as other exponents. One reason is that δ is large. So a modest relative error can readily lead to a large absolute error that smears the difference between 14 and 15. Also corrections to scaling may matter [20,21]. Note that measurement of other critical exponents, η for instance, can also give rise to δ from scaling laws. But the presence of an external field that is the origin of the introduction of δ is more directly and we shall only adhere to this case. Early series expansion results were $\delta = 15.0(4)$ and 15.8(8) for $q=3$ and 4, respectively, with a conclusion that δ was independent of q [30]. An improved result by a higher-order expansion for $q=3$ was $\delta = 15.0(1.5)$ [31], which did not help to solve the problem. Neither did results from a Kadanoff variation real-space RG method that were around 15 but with no estimated errors both for $q=3$ and 4 [32,33]. A first Monte Carlo (MC) RG (MCRG) for the three-state Potts model yielded 15.26(60) [34]. A subsequent systematic MCRG study produced, despite a better value for $q=3$, slow convergence exponents for $q=4$ with the best values of 10.63 and 12.70 with and without introducing vacancies [35], respectively, which were concluded to be still a long way to the conjectured value. Further, an early MC study led to $\delta = 10.8(7)$ for the $q=3$ Potts model [36]. Thus, it is desirable to determine δ using modern techniques.

Another issue is about *weak universality* [37], in which the so-called *reduced* exponents, i.e., exponent ratios instead of exponents themselves, are identical. This is equivalent to the proposition of the universality of the static critical exponents η and δ as long as scaling laws hold because, then

$$2(\beta/\nu) + (\gamma/\nu) = d, \quad (\gamma/\nu) = (\beta/\nu)(\delta - 1), \quad (\gamma/\nu) = 2 - \eta, \tag{8}$$

viz., the exponent ratios are also universal. The conjectured exponents of the 2D Potts model together with those of the exact 2D Ising model (see Table IV below) then place $q=2$ and $q=4$ model in the same class but the $q=3$ one only nearly the same since it has a slightly different δ. However, the majority of numerical δ as mentioned above would put all three models in the same class, which again shows the need for determining it.

The idea of weak universality can be generalized to dynamics since the dynamic critical exponent z itself is a reduced exponent [38]. After some early scattered results [38–43], systematic determinations of z for all three values of $q=2,3,4$ yielded almost identical results of about $z = 2.17(4)$ [44] and $z = 2.16(5)$, $z=2.16(4)$, and $z=2.18(3)$, respectively [45], indicating that all the three q models appear to belong to a single dynamic weak universality class. However, recent short-time critical dynamic methods found $z = 2.19$ for $q=3$ [46–48] but apparently distinct $z=2.29$ [26,48] for $q=4$ (see Table III for errors). It is therefore in need again to determine systematically within one method the dynamic critical exponent for the three models to clarify the issue of weak universality.

In order to study these issues, we adapt the FTS method to the Potts model. To this end, we apply a linearly varying external field that couples just to any one Potts state. The order parameter is then defined as the average of that state only instead of the most popularized state that is usually used [8]. To obtain the coercivity, we introduce a nonequilibrium susceptibility and identify the field at its peak with the coercivity. From the FTS of the order parameter, the coercivity,

the hysteresis area and its derivative, we can then determine systematically both static and dynamic critical exponents as well as the critical temperature. In particular, through introduction of the external field, the magnetic exponent can be measured more directly. Moreover, a method is devised to measure more accurately the exponents. We note in passing that we have studied the 2D three-state Potts model using a linearly changing temperature instead of external field but with an extended dynamic MCRG method [28], an approach different from the present one. Note also that we consider here only local dynamics as realized in the single-site Metropolis algorithm [49]. Nonlocal dynamics arisen from algorithms such as Swendsen-Wang [50] or Wolff [51] has a much reduced z and will not be pursued further.

The rest of the paper is organized as follows. We shall briefly summarize the FTS method of obtaining critical properties in Sec. II and then present the model and results in Sec. III. First, the Potts model, the definition of the order parameter and the nonequilibrium susceptibility, along with simulation details are introduced in Sec. III A. Then, the simulation results including their consequence on critical slowing down and a method to extract more accurately the exponents are presented in Sec. III B. Comparison with existing results is made in Sec. III C. An alternative characterization of the weak universality and a possible application of it are also proposed there. A summary is given in Sec. IV.

II. SUMMARY OF THE FTS METHOD

We now summarize the method to obtain critical properties. Details can be found in [5]. In the FTS regime, the external time scale dominates and drives the system off equilibrium. Hysteresis then emerges even at T_c. In order to deal with the circumstance of two variable in Eq. (5), we scan H back and forth with the same rate R to form a hysteresis loop and integrate over H to get its area $A = \oint M dH$. We then obtain from Eq. (5) FTS of the coercivity H_c, A, and its derivative as

$$H_c(\tau, R) = R^{n_H} g_2(\tau R^{-1/\nu r_H}), \tag{9a}$$

$$A(\tau, R) = R^{n'_H} g_3(\tau R^{-1/\nu r_H}), \tag{9b}$$

$$\partial A(\tau, R)/\partial \tau = R^{a_1} g_4(\tau R^{-1/\nu r_H}), \tag{9c}$$

with

$$n_H = \beta \delta / \nu r_H,$$

$$n'_H = \beta(\delta + 1)/\nu r_H,$$

$$a_1 = \beta(\delta + 1)/\nu r_H - 1/\nu r_H, \tag{10}$$

where all g_i are scaling functions.

At $\tau = 0$, exact power laws

$$H_c|_{\tau=0} \propto R^{n_H},$$

$$A|_{\tau=0} \propto R^{n'_H},$$

$$\partial A/\partial \tau|_{\tau=0} \propto R^{a_1}, \tag{11}$$

follow, from which n_H, n'_H, and a_1 can be determined. The critical temperature can also be determined by finding the minimum deviation from the power-law behavior. Combining the exponents found with the hyperscaling law $\beta(\delta+1) = d\nu$, one can calculate all the static and dynamic critical exponents from

$$\delta = n_H/(n'_H - n_H), \quad \beta/\nu = d(n'_H - n_H)/n'_H,$$

$$z = d(1 - n_H)/n'_H, \quad r_H = d/n'_H,$$

$$\beta = (n'_H - n_H)/(n'_H - a_1), \quad \nu = n'_H/d(n'_H - a_1). \tag{12}$$

Note that in Eqs. (12) the first two lines require only n_H and n'_H, while the last line needs a_1.

III. MODEL AND RESULTS

A. Potts model

The Hamiltonian of the Potts model in the presence of an external field H along the first direction is

$$\mathcal{H} = -\frac{J}{k_B T} \sum_{\langle i,j \rangle} \delta_{\sigma_i, \sigma_j} - \frac{H}{k_B T} \sum_i \delta_{\sigma_i, 1}, \tag{13}$$

where the spin at site i of a 2D lattice, σ_i, can take q states from 1, 2, to q, k_B is Boltzmann's constant, and δ is the Kronecker delta function. In Eq. (13), the first summation runs over all the nearest-neighbor spin pairs and the second over all spins. We shall adopt a unit in which $k_B = J = 1$ for simplicity. Thus the critical point in the absence of H is [7]

$$T_c = 1/\ln(1 + \sqrt{q}), \tag{14}$$

which is in fact a multicritical point [52].

We define the order parameter as

$$M = \left\langle \frac{N_1}{N} \right\rangle = \left\langle \frac{1}{N} \sum_i \delta_{\sigma_i, 1} \right\rangle, \tag{15}$$

namely, the average number of the first state, instead of the usual definition

$$M' = \left\langle \frac{q N_{max}/N - 1}{q - 1} \right\rangle, \tag{16}$$

where N is the total number of spins and $N_{max} = \max(N_1, N_2, \ldots, N_q)$, with N_q representing the number of spins in state q, because it is M not M' that conjugates thermodynamically to the field H and should thus assume the scaling form Eq. (5) although the Potts model and the φ^4 model are not in the same universality class. To obtain usual hysteresis loops, one may rescale the order parameter by

$$m = 2M - 1, \tag{17}$$

which expands the range of values from $M \in [01]$ to $m \in [-11]$.

To attain the coercivity, a simple way may be to take as usual the field H at $m = 0$. This would incur, however, sys-

tematic corrections because the true order parameter $M = 1/2$ at $m=0$ and thus Eq. (9a) would become

$$H_c(\tau, R) = R^{n_H} g_2(\tau R^{-1/\nu r_H}, (1/2) R^{-\beta/\nu r_H}), \qquad (18)$$

which has one more argument proportional to M and thus introduces corrections to scaling even at $\tau = 0$. To overcome this, we utilize a nonequilibrium susceptibility χ that is defined as

$$\chi = (\langle N_1^2 \rangle - \langle N_1 \rangle^2)/N, \qquad (19)$$

which exhibits at the transition a peak whose position then defines the coercivity. Because of the vanishing derivative at the peak, no corrections have to be considered at T_c.

We use the usual Metropolis algorithm [49] with sequential sampling. The lattice used is 512×512 with periodic boundary conditions. We have checked that for that large lattice size, smaller lattices like 256×256 only enlarge fluctuations but yield nearly identical results. However, too small lattices might show finite-size effects and extrapolations might be needed for accurate results. For each finite-time scale proportional to R^{-1}, 100 independent samples are used for average. Larger sample sizes increase, of course, statistical properties of the results, while sufficiently small rates are essential for accuracy. This has several reasons. First, R must not be too large; otherwise the external time scale set by R^{-1} is not long enough as compared to microtime scales for dynamic scaling to emerge. Also for large rates, their large hysteresis overwhelm the small ones and thus affect the fitting. Moreover, as mentioned in the introduction, whereas at T_c, the FTS regime extends to all small enough rates as t_{eq} diverges, it ends roughly to the crossover line $|\tau| R^{-1/\nu r_H} \sim 1$ beyond which the FTS fails. Accordingly, using small rates will increase the precision for determining at least the critical point [5].

In order to obtain good hysteresis loop areas, the initial conditions need special attention. This is because although state 1 is energetically favored or disfavored by the external field, the other states are degenerate. Different populations of these other states change the total energy of the system due to the interfacial energy among them and may thus affect the value of the order parameter M and hence the closing of hysteresis loops. For these reasons, we start with a state in which all sites are set to state 1 at $H=-H_0$ that should be chosen to be sufficiently large for the order parameter to be saturated and the hysteresis loop to close but has been checked not to affect scaling otherwise. After thousands of MC steps per spin (the time units) at that field for equilibration, the field is swept forward and then backward according to $H = \mp H_0 \pm Rt$ to form a hysteresis loop. We found that the equilibrated configuration obtained possesses similar number of the other states besides the first one, a configuration which did not minimize energy but retraceable possibly because of the high temperatures used.

B. Simulation results

Figure 1 shows examples of hysteresis loops of H vs m at T_c. The data points denoted by symbols have been sifted for clarity. When H is positive and large, state 1 is energetically
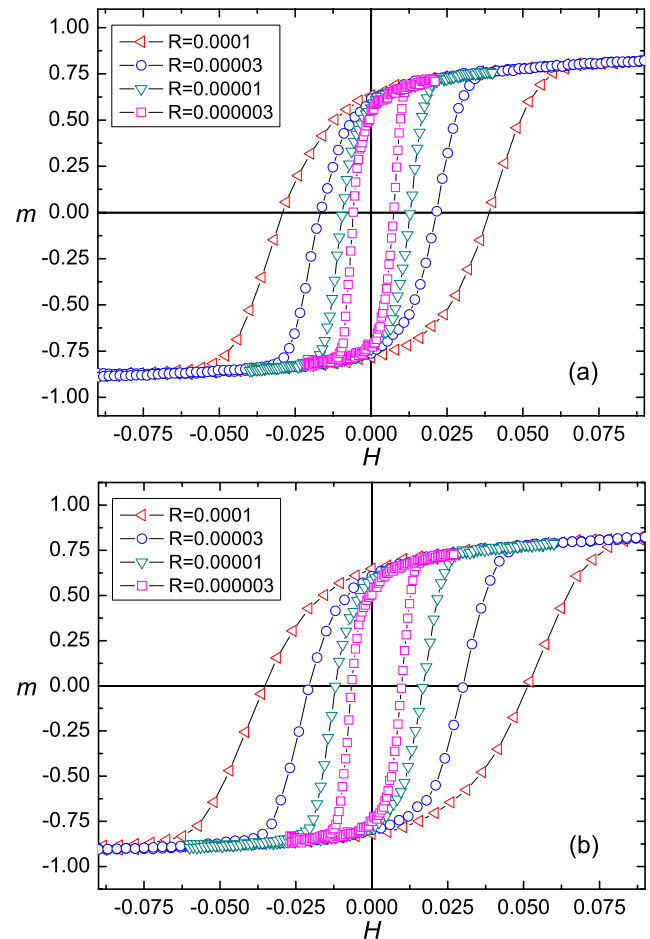
FIG. 1. (Color online) The hysteresis loops of the 2D (a) $q=3$ and (b) $q=4$ Potts models at $T=0.995$ and $T=0.910$, respectively, for several sweep rates R. Lines connecting symbols are only a guide to the eye.

favored and M and m close 1; while for negative and large H, other states than 1 are favored and M is small. A transition that is of concern here then takes place at $H=0$ at equilibrium ($R=0$) but at H_c (near $m=0$) when driving. Note that there are stationary states that are independent of R for positive and negative fields beyond the transition region that scales with R. Figure 2 displays the hysteresis loops for different T at the same R. Generally, the higher the temperature, the smaller the hysteresis loops. One sees from Figs. 1 and 2 that all the hysteresis loops appear in fact similar in the vicinity of T_c. They show clearly that in the present case of nonequilibrium driving, the system subjects a crossover from an equilibriumlike to a FTS regime. In the stationary states that are far from the critical point at $H=0$, the correlation time of the system is short compared to R^{-1} and thus it is controlled by the correlation time instead of R^{-1} and equilibrates quickly and hence is equilibriumlike and follows Eq. (7) if it is still in the critical region. While in the transition region, the system is controlled by the effective finite time scale R^{-1}. The longer it is, the closer the system comes toward the equilibrium state because it has longer time to equilibrate. Eventually, if $R=0$, no hysteresis would appear at all, and Eq. (7) is followed again.
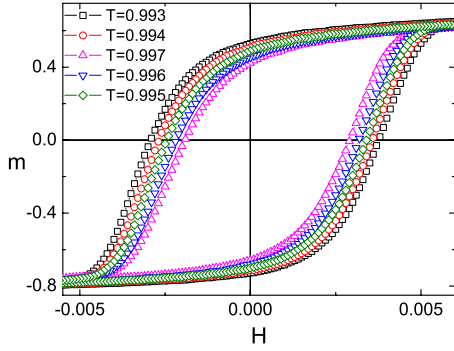
FIG. 2. (Color online) The hysteresis loops of the 2D $q=3$ Potts model at $R=5\times10^{-7}$ for various Ts in the vicinity of T_c. Lines connecting symbols are only a guide to the eye.

As all hysteresis loops behave similar, T_c appears now not special. Neither is critical slowing down a problem. In fact, it is now converted into a controllable process. The FTS regime is defined by $|\tau|R^{-1/r\nu}\lesssim 1$ or $H_{eq}R^{-1}/t_{eq}\lesssim 1$ as pointed out in Sec. I. To probe deep in the asymptotic region where $t_{eq}\gg 1$, one should use a large R^{-1} or small R, which means a long time, although the field H is small from Fig. 1. This is because although the hysteresis characterized by H_c decreases with R as $H_c\sim R^{n_H}$, if it is measured in terms of the time $t_c\equiv H_c/R$, $t_c\sim R^{-(1-n_H)}$, i.e., increases with R^{-1} since $n_H<1$. The long time required by a small R is, however, controllable because a prescribed H is reached at $t=(H-H_0)/R$, where H_0 is the field at $t=0$. Therefore, the linear driving has converted the critical slowing down into a somehow visible process.

Figure 3 demonstrates the peaks of the susceptibility for several rates. The data points shown have also been sifted for clarity. The peaks moves to low fields (absolute values) and increase their heights with R^{-1} or long relaxation times reasonably. When $R=0$, crossover to equilibrium occurs in which the two peaks of a same rate, and in fact, all the peaks shown should merge into a single peak with its height diverging in the thermodynamic limit. One sees that distinct to the Ising cases [5], the peaks are not symmetry for the ascending- and descending-field processes, with the former higher than the latter. This may reflect the fact that when the field is increasing, the single state 1 is always favored. But when the field is decreasing, all other states may compete. In addition, the Potts model is inherently asymmetry as it contains a cubic term [8].

Dependences of A on R and T for $q=3$ and $q=4$ are presented in logarithmic scales in Figs. 4(a) and 4(b), respectively. One sees that similar to the Ising model [5], A decreases reasonably with increasing T and the time scale R^{-1}.

FIG. 3. (Color online) The susceptibility χ/N versus H of the 2D (a) $q=3$ and (b) $q=4$ Potts models at $T=0.995$ and $T=0.910$, respectively, for several sweep rates R. Lines connecting symbols are only a guide to the eye.

Near T_c, the relation between A and R is almost linear, but it curves up and down below and above T_c, respectively, for small Rs. Deviations from the power law between A and R when T varies are given in Table I. The minimum deviation appears at $T=0.995$ for $q=3$ and $T=0.910$ for $q=4$, which are consistent with the known $T_c=0.99497$ and $T_c=0.91024$, respectively, from Eq. (14). Their precisions are thus 0.001 which is the temperature interval we used.

C. Static and dynamic critical exponents

Having determined T_c, we could then proceed as previous [5] to measure n'_H, n_H, and a_1 from the slopes of A, H_c, and $\partial A/\partial\tau$ versus R, respectively, at $T_c=0.995$ for $q=3$ and

TABLE I. Standard deviations (SD$\times10^{-8}$) to the power-law behavior as T varies around T_c for $q=3$ and $q=4$.

$q=3$	T	0.993	0.9994	0.9995	0.996	0.997
	SD	18.129	13.174	5.4197	6.9307	10.629
$q=4$	T	0.908	0.909	0.910	0.911	0.912
	SD	122.08	78.809	49.641	58.939	88.022
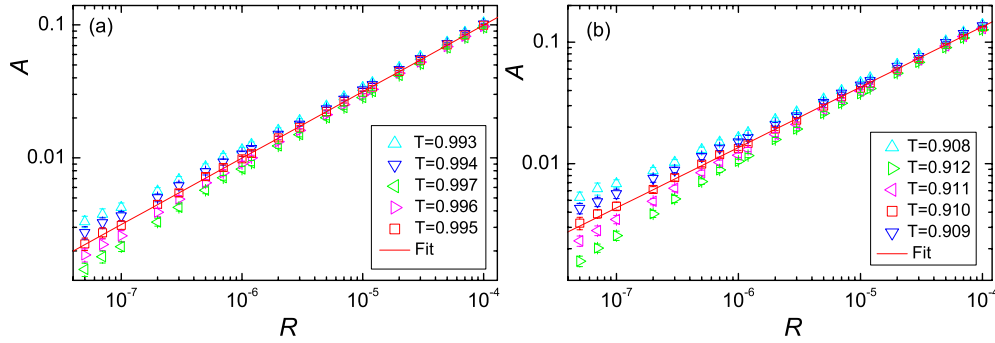
FIG. 4. (Color online) The hysteresis area A plotted with error bars versus R in logarithmic scales for 2D (a) $q=3$ and (b) $q=4$ Potts model. Lines are linear fits at $T_c=0.995$ and $T_c=0.910$ for $q=3$ and $q=4$, respectively.

$T_c=0.910$ for $q=4$ in logarithmic scales as illustrated in Fig. 5. We have used differences at $T=0.993$ and $T=0.997$ for $q=3$ and $T=0.909$ and $T=0.911$ for $q=4$ to approximate the derivatives. Owing to the statistical errors of A and H_c, the slopes of such direct fits would yield, however, poor results of critical exponents albeit with high precisions. This may be appreciated from Fig. 6, in which we plot n vs y_0 of fits to $y=y_0+aR^n$, where y denotes A, H_c, or $\partial A/\partial \tau$. Each data point in it is obtained by neglecting sequentially the largest rate of the remaining data and occasionally also one or two smallest rate(s) for rectification. For example, if we have a series of R in ascending order R_1, R_2, ..., R_s, n_i and y_{0i} are obtained by fitting those data with R from R_1 to R_{s-i+1}. Note that the data points do not appear, however, in this order in Fig. 6. Nevertheless, they fall generally onto a line at least near $y_0=0$ in each subfigure, appearing to justify the method. The only exception is Fig. 6(d), in which the data points bifurcate near $y_0=0$ for a lot of points, which we thus keep and fit without neglecting any point. The relatively wide range of n in Fig. 6 reflects the sensitivity of the fits and also the statistical errors.

Accordingly, our method to extract n'_H, n_H, and a_1 more accurately is then to fit the data points shown in Fig. 6 by polynomials. The exponents are then identified from the fits (lines through data points in Fig. 6) with the values at $y_0=0$ indicated by the vertical lines, and their respective errors estimated from the maximum out of the fits and the root mean square of all the data. This may overestimate the precision of the results. As an evidence, note that we have not shown the error bars in Fig. 6. This is because if they were

shown, they would fill most of the figures because most of them are of the order of magnitudes of the axis scales. As a consequence, fits would be poor.

There is another source of errors. As our chosen T_cs are not equal to the exact ones, the real y_0 for A and H_c may not be exactly zero albeit tiny [6], and the effect of the shift on $\Delta A/\Delta \tau$ may double due to the central difference we used. Yet, even for $T=T_c$, the exact one, finite-size effects may shift the actual T_c off it. Of course, this shift does not just exist here but generally. Fortunately, possibly for the real y_0 may indeed be tiny, our results appear to be quite good, except the $q=4$ a_1 that depends indeed on $\Delta A/\Delta \tau$, since the deviation of our chosen T_c from the real one is bigger for $q=4$ than for $q=3$.

From n_H, n'_H, and a_1, all the critical exponents can be calculated according to Eqs. (12) and are collected in Table II.

D. Comparison with existing results

To compare with existing results, we extend the table compiled in Wu's review paper [8] to Table III. Comparing Tables II and III, one sees reasonable agreement with the conjectured values both for $q=3$ and $q=4$. The only static exponents that escape the error limits are ν of both q and β of $q=4$; but note that the errors may have been underestimated as pointed out above. As mentioned in the previous paper [5], these large deviations stem probably from the error of a_1, which is the most serious one in our method, as it involves derivative [22,53]. Also as mentioned in the last
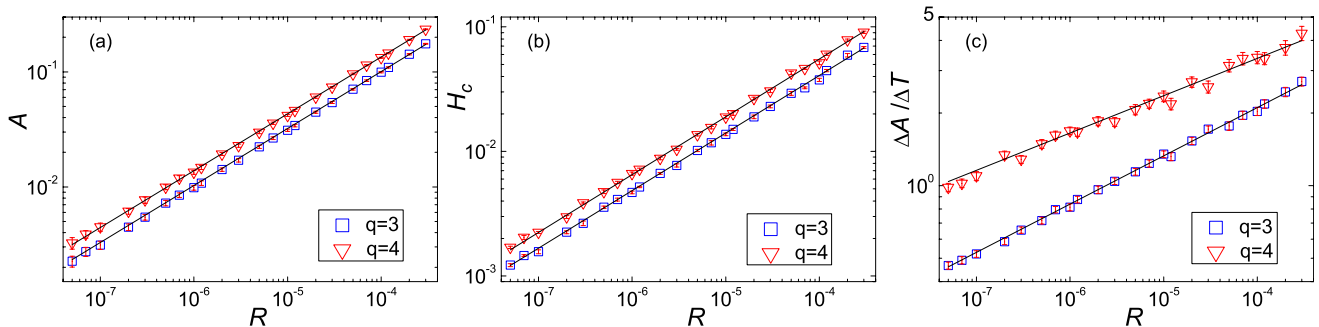
FIG. 5. (Color online) (a) A, (b) H_c, and (c) $\Delta A/\Delta T$ plotted with error bars versus R in logarithmic scales at $T_c=0.995$ and $T_c=0.910$ for $q=3$ and $q=4$, respectively.
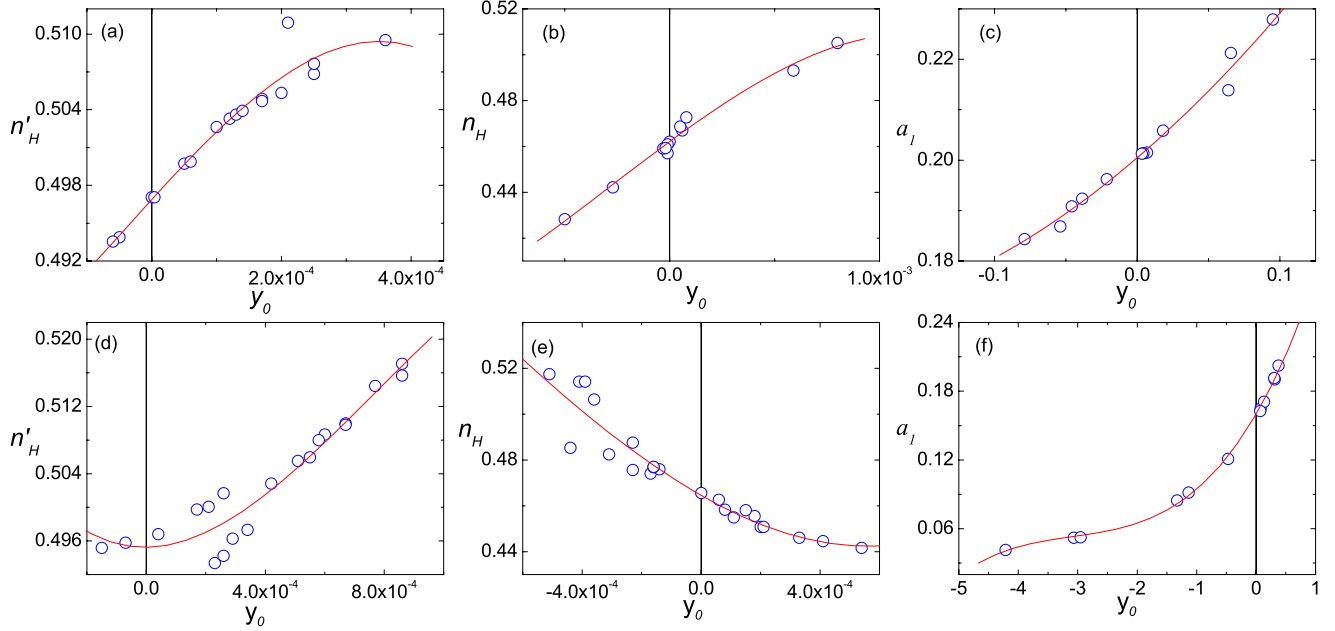
FIG. 6. (Color online) n vs y_0 of fits to $y = y_0 + aR^n$ for the [(a)–(c)] $q=3$ and [(d)–(f)] $q=4$ Potts model at $T_c = 0.995$ and $T_c = 0.910$, respectively. We denote in the figures n for A, H_c, and $\Delta A / \Delta T$ directly as n'_H, n_H, and a_1, respectively, although the latter are only the values at the intersections of the vertical lines at $y_0 = 0$ and the other lines that are fits of the data by cubic polynomials.

subsection, the shift of T_c may affect the accuracy of a_1. As an evidence, note that β/ν of both q behaves well as it is independent of a_1 from Eq. (12). In addition, the relatively large error of δ of $q=4$ arises from the small $(n'_H - n_H)$ factor in the denominator that enlarges every error. Although our measured δs for $q=3$ and $q=4$ still overlaps slightly within the errors, they should nevertheless support their respective conjectured values.

The dynamic critical exponent z obtained for both $q=3$ and $q=4$ agrees well with previous MC simulation results [44,45], and taking together with z of the Ising model measured by the FTS method as listed in Table IV [5] appears to confirm the dynamic weak universality that the Potts model with $q=2$, $q=3$, and $q=4$ all share the same z but not to support the short-time dynamic results [26,48]. Note that although the relative errors of β and ν of $q=4$ are almost up to 9%, they should mostly stem from the error of a_1 as mentioned above. The relative errors of other quantities including z that do not contain a_1 are small. However, the relative error of 2.16 and 2.29 is about 5–6 %, just near the verge of the present precision of the other quantities. So, overlap of the two zs seems unlikely albeit not exclusive. More work is, therefore, welcome here.

As mentioned in the introduction, static weak universality means δ and η are identical, while dynamic one will suggest z be the same. So, both static and dynamic weak universality will need all the three exponents to be identical. From Eqs. (12) and

$$\eta = 2n_H/n'_H - d, \qquad (20)$$

one sees that these three exponents depend only on n'_H (or r_H) and n_H for the same spatial dimension d. Referring to the values n'_H (or r_H) and n_H for the 2D Ising model [5] listed in Table IV, one finds that all three models with $q=2$, 3, and 4 indeed share the same n'_H (or r_H) and n_H exactly to the second effective digits. However, one knows from the conjectured values that the $q=3$ model has a δ that is different from the other two and thus is not in the same weak universality class. Yet, from Table IV, the reduced exponents are, in fact, quite close though certain exponents themselves may differ a lot, α in particular. Therefore, a possible application of the weak universality hypothesis is to predict quite accurately the reduced exponents and even some exponents themselves of a system whose critical exponents have not been exactly determined but that is already known even roughly to belong to a weak universality class. This latter knowledge will require three exponents δ, η, and z. However, using the present FTS method, one needs just n'_H (or r_H) and n_H with an accuracy of only up to their second effective digits, which may be readily realized.

TABLE II. Measured and derived exponents.

q	n'_H	n_H	a_1	δ	β/ν	β	ν	z	r_H
3	0.4969(12)	0.4624(9)	0.200(10)	13.4(6)	0.139(6)	0.116(5)	0.838(3)	2.164(7)	4.025(10)
4	0.4954(13)	0.4645(21)	0.154(12)	15.1(1.3)	0.124(10)	0.0900(7)	0.726(3)	2.163(10)	4.039(11)

TABLE III. Comparison of various numerical estimates of critical exponents.

q	Method	δ	β	ν	z
3	Conjectured value	14	$1/9=0.11111$	$5/6=0.83333$	
	MC [36]	10.8(7)			
	Kadanoff variational RG [32]	14.48	0.1061		
	Kadanoff variational RG [33]	14.64	0.107	0.837	
	MCRG [34]	15.26(60)	0.101(6)	0.824(10)	
	MCRG [35]	14.38		0.82	
	Migdal RG [38]				1.92
	MC nonlinear relaxation [39]		0.1		2.28
	Dynamic MCRG [40,41]				2.7(4)
	FSS [42]				2.2(1)
	Dynamic MCRG [43]				2.43(15)
	Extended dynamic MCRG [28]		0.108(4)	0.816(27)	2.171(62)
	Series expansion [30]	15.0(4)	0.105(5)		
	Series expansion [31]	15.5(1.5)	0.1064		
	MC equilibrium relaxation time [44]				2.17(4)
	MC magnetization relaxation [45]				2.16(4)
	Density-Matrix RG [24]		0.1112(1)	0.8333(8)	
	Short-time dynamics [22]		0.107(6)	$[1.24(3)]^{-1}$	2.196(8)
	Short-time dynamics [46]				2.196(8)
	Short-time dynamics [47]				2.191(6)
	Short-time dynamics [48]				2.197(3)
	Nonequilibrium critical relaxation [29]		0.1080(20)	$[1.213(6)]^{-1}$	2.1735(40)
	FTS (this work)	13.4(6)	0.116(5)	0.838(3)	2.164(7)
4	Conjectured value	15	$1/12=0.08333$	$2/3=0.66667$	
	Kadanoff variational RG [33]	15.53			
	MCRG with vacancies [35]	10.6		0.75	
	MCRG without vacancies [35]	12.70		0.75	
	Dynamic MCRG [43]				2.36(20)
	Migdal RG [38]				2.0
	MC nonlinear relaxation [39]				2.85
	Series expansion [30]	15.8(8)			
	MC equilibrium relaxation time [44]				2.17(4)
	MC magnetization relaxation [45]				2.18(3)
	Density-Matrix RG [24]		0.0795(37)	0.662(13)	
	Short-time dynamics [25,48]		0.0836(2)	0.667(1)	2.290(3)
	Short-time dynamics [26]		0.0830(6)	0.669(6)	2.294(3)
	FTS (this work)	15.1(1.3)	0.0900(7)	0.726(3)	2.163(10)

These remarks on the weak universality lead to a further conclusion. Whereas determining a weak universality class may only require an accuracy of up to two effective digits of n'_H (or r_H) and n_H, at least three are needed to accurately determine the critical exponents themselves.

IV. SUMMARY

We have adapted the FTS method to the 2D $q=3$ and $q=4$ Potts models to determine systematically their critical properties, their magnetic critical exponent δ and dynamic critical exponent z in particular. To this end, we have applied for the first time a linearly varying external field to the Potts model that couples to one of its q states to manipulate its dynamics in the vicinity of its T_c and defined the order parameter other than the usual one and the nonequilibrium susceptibility to extract the coercive fields. The applied field drives the system out of equilibrium and thus produces hysteresis. From the FTS of the order parameter, the coercivity, and the hysteresis area and its derivative, we can then determine both static and dynamic critical exponents as well as the critical temperature. The static critical exponents obtained in general and δ in particular agree reasonably with the conjectured ones. The dynamic critical exponents ob-

TABLE IV. Critical exponents of the Potts model with $q = 2$, 3, and 4.

q	δ	η	β/ν	γ/ν	β	ν	γ	α	z	r_H	n'_H	n_H
2	15	1/4	1/8	7/4	1/8	1	7/4	0	2.154(11)	4.028(15)	0.4965(18)	0.4653(19)
3	14	4/15	2/15	26/15	1/9	5/6	13/9	1/3	2.164(7)	4.025(10)	0.4969(12)	0.4624(9)
4	15	1/4	1/8	7/4	1/12	2/3	7/6	2/3	2.163(10)	4.039(11)	0.4954(13)	0.4645(21)

tained appear to confirm the proposed dynamic weak universality that the Potts model with $q = 2$ (Ising model), $q = 3$, and $q = 4$ all share the same z of about 2.17. This, however, unlikely to agree with recent short-time dynamic results for $q = 4$ and thus calls for further studies. The simulation results also show that critical slowing down does not appear in FTS directly but has been converted into visible processes of running small Rs.

We have proposed to use the exponents n'_H (or r_H) and n_H as a more convenient token for defining weak universality because for a system to be in a weak universality class, it may possibly require these exponents to have an accuracy to just two effective digits, which can be readily obtained. Of course, more digits are demanding for accurately determining the critical exponents.

The theory and results of the present work therefore show that the FTS can be as effective as the usual FSS.

ACKNOWLEDGMENT

[1] M. E. Fisher and A. E. Ferdinand, Phys. Rev. Lett. **19**, 169 (1967); M. E. Fisher and M. N. Barber, *ibid.* **28**, 1516 (1972); *Finite Size Scaling*, edited by J. Cardy (North-Holland, Amsterdam, 1988); *Finite Size Scaling and Numerical Simulation of Statistical Systems*, edited by V. Privman (World Scientific, Singapore, 1990); F. M. Gasparini, M. O. Kimball, K. P. Mooney, and M. Diaz-Avila, Rev. Mod. Phys. **80**, 1009 (2008).

[2] D. J. Amit and V. Martin-Mayor, *Field Theory, the Renormalization Group, and Critical Phenomena*, 3rd ed. (World Scientific Press, Singapore, 2005).

[3] D. P. Landau and K. Binder, *A Guide to Monte Carlo Simulations in Statistical Physics*, 2nd ed. (Cambridge University Press, Cambridge, 2005).

[4] E. Brézin, J. Phys. **43**, 15 (1982); E. Brézin and J. Zinn-Justin, Nucl. Phys. B **257**, 867 (1985).

[5] S. Gong, F. Zhong, X. Huang, and S. Fan, New J. Phys. **12**, 043036 (2010); the idea of finite-time scaling was once used in simulated annealing [S. Shinomoto and Y. Kabashima, J. Phys. A **24**, L141 (1991)] and forced oscillations [K. Hukushima and K. Nemeto, J. Phys. Soc. Jpn. **64**, 1863 (1995); H. Shima and T. Nakayama, *ibid.*, **67**, 2189 (1998); Phys. Rev. B **60**, 14066 (1999)] nearly two decades ago but was not put forward as a systematically concept and lacked a systematic theory.

[6] F. Zhong, Phys. Rev. B **66**, 060401(R) (2002); F. Zhong and Z. F. Xu, *ibid.* **71**, 132402 (2005); F. Zhong, Phys. Rev. E **73**, 047102 (2006).

[7] R. B. Potts, Proc. Cambridge Philos. Soc. **48**, 106 (1952); for examples of recent applications, see S. N. Dorogovtsev, A. V. Goltsev, and J. F. F. Mendes, Eur. Phys. J. B **38**, 177 (2004); S. Coutinho, W. A. M. Morgado, E. M. F. Curado, and L. da Silva, Phys. Rev. B **74**, 094432 (2006).

[8] F. Y. Wu, Rev. Mod. Phys. **54**, 235 (1982).

[9] R. J. Baxter, Phys. Today **58**(12), 15 (2005).

[10] R. J. Baxter, J. Phys. C **6**, L445 (1973).

[11] M. P. M. den Nijs, J. Phys. A **12**, 1857 (1979).

[12] R. B. Pearson, Phys. Rev. B **22**, 2579 (1980); B. Nienhuis, E. K. Riedel, and M. Schick, J. Phys. A **13**, L189 (1980).

[13] R. J. Baxter, J. Phys. A **13**, L61 (1980).

[14] R. J. Baxter and F. Y. Wu, Phys. Rev. Lett. **31**, 1294 (1973); R. J. Baxter, M. F. Sykes, and M. G. Watt, J. Phys. A **8**, 245 (1975).

[15] S. Alexander, Phys. Lett. A **54**, 353 (1975).

[16] I. G. Enting, J. Phys. A **8**, L35 (1975); E. Domany and E. K. Riedel, J. Appl. Phys. **49**, 1315 (1978).

[17] V. S. Dotsenko, Nucl. Phys. B **235**, 54 (1984); D. Friedan, Z. Qiu, and S. Shenker, Phys. Rev. Lett. **52**, 1575 (1984); J. L. Cardy, in *Phase Transitions and Critical Phenomena*, edited by C. Domb and J. L. Lebowitz (Academic, New York, 1987), Vol. 11.

[18] J. L. Black and V. J. Emery, Phys. Rev. B **23**, 429 (1981).

[19] M. P. Nightingale and H. W. J. Blöte, Physica A **104**, 352 (1980); H. W. J. Blote, M. P. Nightingale, and B. Derrida, J. Phys. A **14**, L45 (1981).

[20] M. Nauenberg and D. J. Scalapino, Phys. Rev. Lett. **44**, 837 (1980); J. L. Cardy, M. Nauenberg, and D. J. Scalapino, Phys. Rev. B **22**, 2560 (1980).

[21] J. Salas and A. D. Sokal, J. Stat. Phys. **88**, 567 (1997).

[22] L. Schülke and B. Zheng, Phys. Lett. A **204**, 295 (1995); **215**, 81 (1996).

[23] J. Salas and A. D. Sokal, J. Stat. Phys. **87**, 1 (1997).

[24] E. Carlon and F. Iglói, Phys. Rev. B **57**, 7877 (1998).

[25] R. da Silva and J. R. Drugowich de Felício, Phys. Lett. A **333**, 277 (2004).

[26] H. A. Fernandes, E. Arashiro, J. R. Drugowich de Felício, and A. A. Caparica, Physica A **366**, 255 (2006).

[27] A. S. Anjos, D. A. Moreira, A. M. Mariz, and F. D. Nobre, Phys. Rev. E **74**, 016703 (2006).

[28] S. Fan and F. Zhong, Phys. Rev. E **76**, 041141 (2007).

[29] K. Nam, B. Kim, and S. J. Lee, Phys. Rev. E **77**, 056104

(2008).

[30] I. G. Enting, J. Phys. A **7**, 1617 (1974).

[31] S. Miyashita, D. D. Betts, and C. J. Elliot, J. Phys. A **12**, 1605 (1979).

[32] T. W. Burkhardt, H. J. F. Knops, and M. den Nijs, J. Phys. A **9**, L179 (1976).

[33] C. Dasgupta, Phys. Rev. B **15**, 3460 (1977).

[34] R. H. Swendsen, Phys. Rev. Lett. **42**, 859 (1979).

[35] C. Rebbi and R. H. Swendsen, Phys. Rev. B **21**, 4094 (1980).

[36] B. L. Arora and D. P. Landau, in *18th Conference on Magnetism and Magnetic Materials, Denver 1972*, AIP Conf. Proc. No. 10, edited by C. D. Graham, Jr., and J. J. Rhyne (AIP, New York, 1973), p. 870.

[37] M. Suzuki, Prog. Theor. Phys. **51**, 1992 (1974).

[38] G. Forgacs, S. T. Chui, and H. L. Frisch, Phys. Rev. B **22**, 415 (1980).

[39] K. Binder, J. Stat. Phys. **24**, 69 (1981).

[40] J. Tobochnik and C. Jayaprakash, Phys. Rev. B **25**, 4893 (1982).

[41] M. Aydin and M. C. Yalabik, J. Phys. A **17**, 2531 (1984).

[42] M. Aydin and M. C. Yalabik, J. Phys. A **18**, 1741 (1985).

[43] L. de Arcangelis and N. Jan, J. Phys. A **19**, L1179 (1986).

[44] S. Tang and D. P. Landau, Phys. Rev. B **36**, 567 (1987).

[45] O. F. de Alcantara Bonfim, Europhys. Lett. **4**, 373 (1987).

[46] K. Okano, L. Schulke, K. Yamagishi, and B. Zheng, Nucl. Phys. B **485**, 727 (1997).

[47] J. B. Zhang, L. Wang, D. W. Gu, H. P. Ying, and D. R. Ji, Phys. Lett. A **262**, 226 (1999).

[48] R. da Silva, N. A. Alves, and J. R. Drugowich de Felício, Phys. Lett. A **298**, 325 (2002).

[49] N. Metropolis, A. W. Rosenbluth, M. N. Rosenbluth, A. M. Teller, and E. Teller, J. Chem. Phys. **21**, 1087 (1953).

[50] R. H. Swendsen and J. S. Wang, Phys. Rev. Lett. **58**, 86 (1987).

[51] U. Wolff, Phys. Rev. Lett. **62**, 361 (1989).

[52] J. P. Straley and M. E. Fisher, J. Phys. A **6**, 1310 (1973).

[53] Z. B. Li, L. Schülke, and B. Zheng, Phys. Rev. Lett. **74**, 3396 (1995); B. Zheng, Int. J. Mod. Phys. B **12**, 1419 (1998).